Appl. Phys. B 84, 265–267 (2006)
DOI: 10.1007/s00340-006-2328-5

Applied Physics B
Lasers and Optics

T. YATSUI[1,✉]
Y. NAKAJIMA[2]
W. NOMURA[2]
M. OHTSU[1,2]

High-resolution capability of optical near-field imprint lithography

[1] Solution-Oriented Research for Science and Technology (SORST), Japan Science and Technology Agency, 687-1 Tsuruma, Machida, Tokyo, 194-0004, Japan
[2] School of Engineering, The University of Tokyo, 7-3-1 Hongo, Bunkyo-ku, Tokyo, 113-8656, Japan

Received: 15 December 2006/Revised version: 2 May 2006
Published online: 22 June 2006 • **© Springer-Verlag 2006**

ABSTRACT We propose a novel method to increase the resolution of imprint lithography by introducing strong localization of the optical near-field intensity, depending on the mold structure. By optimizing the thickness of the metallic film on a SiO_2 line-and-space (LS) mold without a sidewall coating, we confirmed that the optical near-field strongly localizes at the edge of the mold, using a finite-difference time-domain calculation method. Based on the calculated results, we performed optical near-field imprint lithography using a mold with metallized (20-nm-thick Al without a sidewall coating) SiO_2 LS with a 300-nm half-pitch that was 200-nm deep with illumination using the g-line ($\lambda = 436$ nm), and obtained features as narrow as 50 nm wide.

PACS 81.16.Nd; 81.16.Rf

1 Introduction

As next-generation lithography (NGL) for the 32-nm node and below, ArF immersion lithography, extreme ultraviolet lithography (EUVL), and electron projection lithography (EPL) have been studied. However, a practical problem is the increasing cost and size of NGL tools. To solve these problems, optical near-field lithography has been developed by introducing tri-layer resist. The fabrication of sub-50 nm features has been realized using the i-line ($\lambda = 365$ nm) [1], with conventional photolithography facilities.

A further decrease in feature size has been reported with the introduction of imprint lithography [2], which resulted in the fabrication of 14-nm pitch features [3]. Although conventional imprint lithography results in the same mold structure, the use of the optical near-field intensity distribution should realize features smaller than the mold structure, since a nano-scale mold has a nano-scale optical field distribution at its edge.

✉ Fax: +81-42-788-6031, E-mail: yatsui@ohtsu.jst.go.jp

In this study, we propose and demonstrate optical near-field imprint lithography to introduce its ability to obtain a higher resolution than the size of the mold features.

2 Optimizing the mold structure

To realize the efficient excitation of an optical near-field on a mold, the thickness of the metallic film and the coverage were optimized using the finite-difference time-domain (FDTD) method [4]. For comparison with a conventional photolithographic mask, the optical field distribution for 80-nm half-pitch, 200-nm-deep Cr line-and-space (LS) on the SiO_2 ($n = 1.5$) substrate was calculated at a wavelength of 436 nm (g-line). Here, the refractive index of Cr was assumed to be $n = 1.78 + i2.69$ [5], and the line was parallel to the y-axis (Fig. 1a). Since the imprint mold used in this study was fabricated using SiO_2, we also calculated the optical field distribution of 80-nm half-pitch, 200-nm-deep SiO_2 LS, coated with aluminum film ($n = 0.56 + i5.2$) [5] (Fig. 1b–d). The minimum cell size was $5 \times 12.5 \times 5$ nm.

Figure 1e shows the cross-sectional profile along the x-axis 10 nm from the mold. The optical field intensity distribution of the Cr LS used for conventional photolithography resulted in a single peak corresponding to the space of the Cr mask, which resulted from reducing the optical field intensity through the 200-nm-thick Cr film (curve 1a in Fig. 1e). By contrast, coating the SiO_2 LS with a 20-nm-thick Al film (Fig. 1b and c) enhanced the electric field intensity at the edge of the mold (curves 2a and 3a in Fig. 1e). Higher localization at the edge of the mold was realized without a sidewall coating (Fig. 1b and curve 2a in Fig. 1e). Since this localization was not observed for the thicker coating (a 50-nm-thick Al film on top of SiO_2 and a 20-nm-thick Al film on the sidewall) and was not observed in the y-polarization (curve y in Fig. 1f), this localized optical near-field originated from the edge effect. Since efficient excitation of the surface plasmon is obtained with a 15-nm-thick aluminum coating on glass in the Kretschmann configuration [6], this size-dependent feature is attributed to localized surface plasmon resonance on the Al film. Furthermore, the localization of the optical field intensity to an area as narrow as 25-nm in curve 2a in Fig. 1e

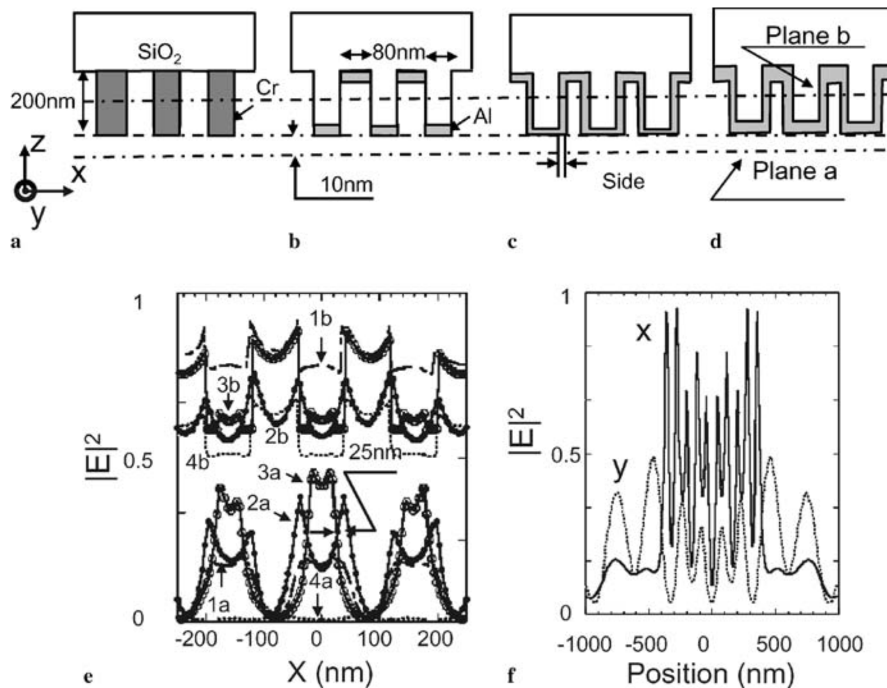

FIGURE 1 Schematic of the calculation models. (**a**) Cr LS on SiO_2 substrate. (**b–d**) SiO_2 LS coated with (b) 20-nm Al without a sidewall coating, (**c**) 20-nm Al with a sidewall coating, and (**d**) 50-nm Al at the top and 20-nm Al on the sidewall. (**e**) Curves 1a–4a show the cross-sectional profiles along the x-axis 10 nm from the mold (plane a) with five grooves in the mold. Curves 1b–4b show the cross-sectional profiles along the x-axis 10 nm from the bottom of the mold (plane b). The beam width at $1/e^2$ of incident light with a Gaussian shape was 1000 nm. The x-coordinate is perpendicular to the grating in (**a–d**). (**f**) The polarization dependence of the cross-sectional profiles for x- (perpendicular to the LS direction) and y- (parallel to the LS direction) polarization for the mold with five grooves in the mold. The beam width at $1/e^2$ of incident light with a Gaussian shape was 2000 nm ($1/e^2$)

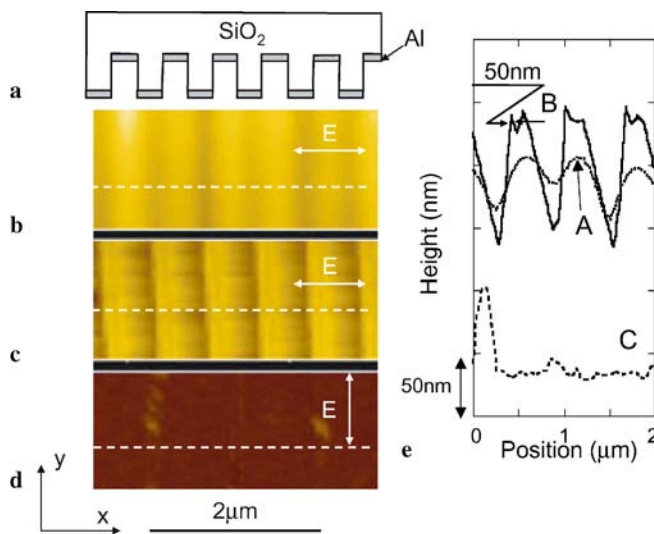

FIGURE 2 (**a**) Mold position before its release from PAK01. (**b–d**) show AFM images of the surface of the PAK01 using a bare mold with x-polarization (perpendicular to the LS direction), an Al-coated mold with x-polarization, and an Al-coated mold with y-polarization (parallel to the LS direction), respectively. (**d**) Curves A, B, and C show the cross-sectional profiles along the *dashed white lines* in (**b**), (**c**), and (**d**), respectively

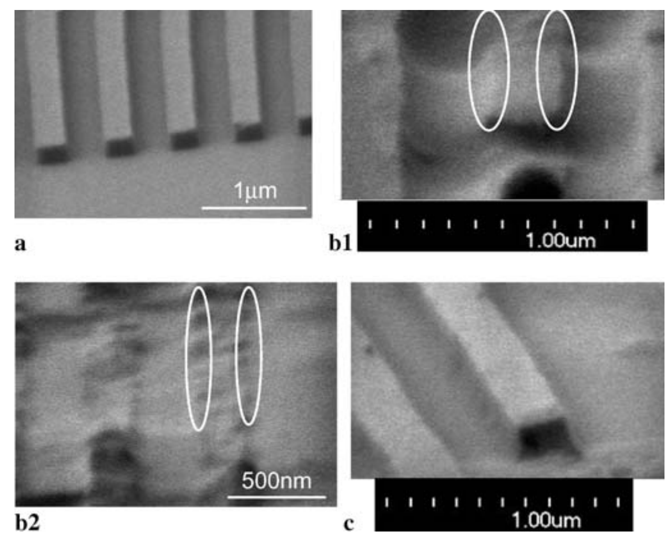

FIGURE 3 Tilted (30°) SEM images using (**a**) a bare mold with x-polarization (perpendicular to the LS direction), (**b**.1) (**b**.2) an Al-coated mold with x-polarization, and (**c**) an Al-coated mold with y-polarization

infers the realization of a resolution higher than the mold size. This localization was also observed in curve 2b (Fig. 1e) obtained in the plane along the x-axis 10 nm from the bottom of the mold.

3 Experiment

We performed imprint lithography to confirm the higher resolution capability using an optical near-field, as discussed above. Commercial photocurable acryl PAK01 resin (blended by Toyo Gosei) was used; it is composed of tri-propylene-glycol-diacrylate monomer with dimethoxy-phenyl-acetophenon as the photo-initiator and has good release properties [7]. Polycarbonate (PC) substrate was spin-coated with PAK01. We used 300-nm half-pitch, 200-nm-deep SiO_2 LS as the mold.

To obtain the optimum structure shown in Fig. 1b (20-nm-thick Al film with no sidewall coating), the mold was coated with Al using vacuum evaporation (Fig. 2a). The mold was pressed into the liquid polymer on PC substrate under a pressure of 70 kPa using a conventional contact mask aligner (MJB3, SUSS MicroTec KK). It was irradiated with UV light (g-line: 436 nm, power density: 30 mW/cm^2) for 30 s from the back of the mold, while maintaining the imprint pressure during exposure. After pressing the mold and UV curing, we separated the PC substrate from the mold, and the pattern was transferred.

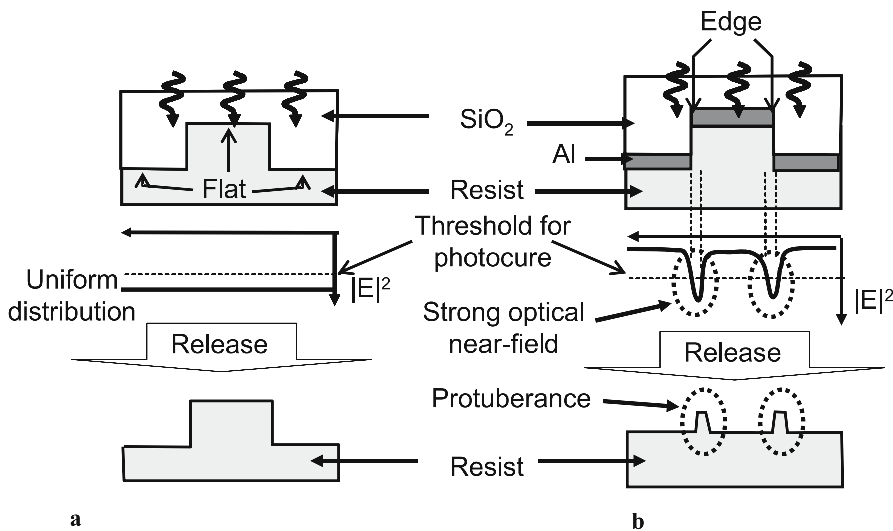

FIGURE 4 Schematics of (**a**) conventional imprint lithography and (**b**) optical near-field imprint lithography

4 Results and discussion

First, we obtained topographic atomic force microscopy (AFM) images of the surface of PAK01 after release of the mold. Figure 2b–d show AFM images of a bare SiO_2 mold with x-polarization (perpendicular to the LS direction), an Al-coated SiO_2 mold with x-polarization, and an Al-coated SiO_2 mold with y-polarization (parallel to the LS direction), respectively. Although the bare mold resulted in a single pitch corresponding to the mold pitch (Fig. 2b and curve A in Fig. 2e), we obtained sharp (50 nm) protruding structures at the edge of the Al-coated SiO_2 mold, when the mold was pressed under x-polarization (Fig. 2c and curve B in Fig. 2e). Although the pitch differs between the numerical and experimental results, these profiles with protruding structures seen at the edge of the Al-coated SiO_2 mold are in good agreement with those calculated using FDTD (curve 2a of Fig. 1e). The calculated value at the point next to the interface is unstable in the FDTD calculation due to the drastic change in the refractive index. Furthermore, since the distribution of the optical near-field along the z-axis is as large as that along the x-axis, the optical near-field is believed to be localized to a region small as 20-nm along the z-axis. Therefore, we compared the profiles at the second point from the interface (10 nm apart from the interface). Although the calculated and obtained profiles differ, the protuberances were obtained only with x-polarization with an Al coating; therefore, we believe that the protuberances originated from the plasmon resonance, as predicted by the FDTD calculation. These results indicate that the resolution was higher than the pitch of the mold.

Next, we obtained scanning electron microscope (SEM) images of the transferred pattern (Fig. 3a–c). As shown in the AFM images, the SEM images confirmed that there were protuberances where the edge of the mold was pressed (inside the white solid ellipses in Fig. 3b.1 and b.2) using the Al-coated mold with x-polarization.

The field distribution calculated using the FDTD method did not predict the resist structure after release of the mold. However, the correspondence between the AFM and SEM images showed that protuberances were formed at positions where a strong optical near-field was localized. Based on these results, we concluded that using conventional imprint lithography, a strong uniform optical field intensity resulted in the formation of the same pitch as that of the mold (Fig. 4a). In contrast, with optical near-field imprint lithography, the resist was deformed in the underexposed condition where the flat surface of the mold was press, which was due to the Al coating of the mold, and the resist was remained in the overexposed condition arising from the strong optical near-field, which was due to the edge effect from where the edge of the mold was pressed. This enhancement originated from the resonant excitation of the surface plasmon on the Al film, which resulted in protuberances smaller than the pitch of the mold (see Fig. 4b). Future evaluations, which will include the effects of power and irradiation time, are required to explain the optimum dose for the higher contrast of the protuberances.

5 Conclusion

We performed optical near-field imprint lithography to increase the resolution over conventional imprint lithography. By introducing local field enhancement of the optical near-field using a metallized LS SiO_2 mold (300-nm half-pitch and 200-nm deep) without sidewall coating, we obtained features as small as 50-nm wide on illumination with the g-line ($\lambda = 436$ nm). The resolution could be increased further by surface treatment with Al or other durable metals or semiconductors.

REFERENCES

1 T. Ito, M. Ogino, T. Yamada, Y. Inao, T. Yamaguchi, T. Mizutani, R. Kuroda, J. Photopoly. Sci. Technol. **18**, 435 (2003)
2 S.Y. Chou, P.R. Krauss, W. Zhang, L. Guo, L. Zhuang, J. Vac. Sci. Technol. B **15**, 2897 (1997)
3 M.D. Austin, H. Ge, W. Wu, M. Li, Z. Yu, D. Wasserman, S.A. Lyon, S.Y. Chou, Appl. Phys. Lett. **84**, 5299 (2004)
4 The computer simulations in this paper are performed by a FDTD-based program, Poynting for Optics, a product of Fujitsu, Japan
5 E.D. Palik (Ed.), *Handbook of Optical Constants of Solids* (Academic, New York, 1985)
6 H. Raether (Ed.), *Surface Plasmons* (Springer-Verlag, Berlin, 1988)
7 J. Haisma, M. Verheijen, K. van den Heuvel, J. van den Berg, J. Vac. Sci. Technol. B **14**, 4124 (1996)